

**An Unusual Topological RNA Architecture with an Eight-Stranded Helical Fragment Containing A-, G- and U-Tetrads**

Chao-Da Xiao,<sup>†</sup> Takumi Ishizuka,<sup>†</sup> Xiao-Qing Zhu,<sup>†</sup> Yue Li,<sup>‡</sup> Hiroshi Sugiyama,<sup>‡</sup> and Yan Xu<sup>†</sup>

<sup>†</sup>Division of Chemistry, Department of Medical Sciences, Faculty of Medicine, University of Miyazaki, 5200 Kihara, Kiyotake, Miyazaki 889-1692, Japan.

<sup>‡</sup>Department of Chemistry, Graduate School of Science, Kyoto University, Kitashirakawa-oiwakecho, Sakyo-ku, Kyoto 606-8502, Japan.

Corresponding Author

\*xuyan@med.miyazaki-u.ac.jp

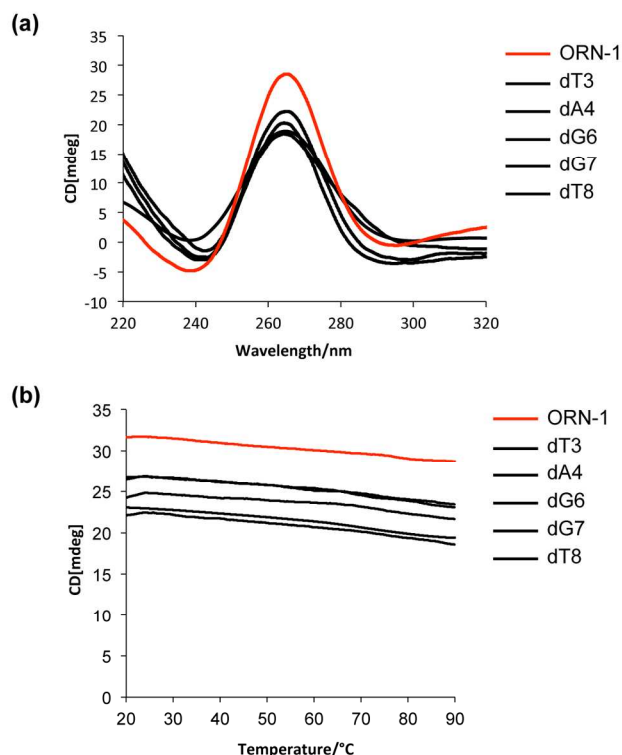


**Figure S1.** (a) CD spectra of ORN-1 (red) and the modified RNA sequences (back) containing a single deoxyribose substitution in Table S1 in the presence of 100 mM NaCl at 25 °C. The similarity of CD spectrum of ORN-1 and the modified RNA sequences indicated that the modification does not affect the RNA structure. (b) The red line shown CD melting curve of ORN-1 monitored at 265 nm. The back lines shown CD melting curves of modified RNA sequences. The modified RNA sequences have similar CD melting curve of ORN-1 indicated that the modification does not affect the stability of RNA structure.

**Table S1.** Modified RNA Sequences Containing a Single Deoxyribose Substitution Used in This Study

	Residue number	1	2	3	4	5	6	7	8
Sequence	8-nt (dT3)	G	U	<b>dT</b>	A	G	G	G	U
	8-nt (dA4)	G	U	U	<b>dA</b>	G	G	G	U
	8-nt (dG6)	G	U	U	A	G	<b>dG</b>	G	U
	8-nt (dG7)	G	U	U	A	G	G	<b>dG</b>	U
	8-nt (dT8)	G	U	U	A	G	G	G	<b>dT</b>

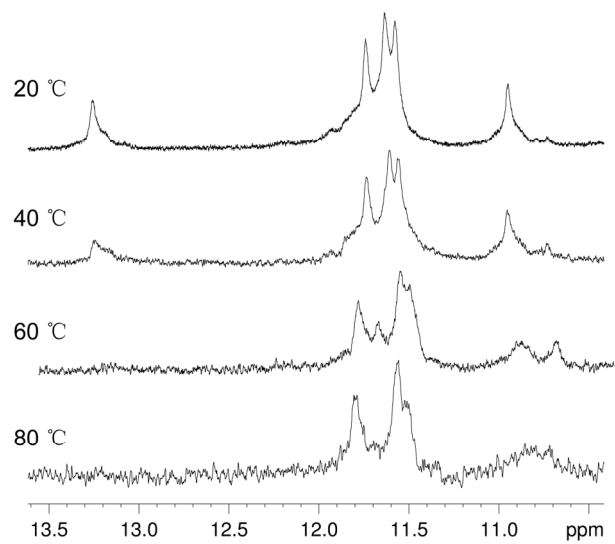


**Figure S2.** Imino proton NMR spectra of ORN-1 at different temperatures in the presence of 100 mM NaCl and 10 mM Na-phosphate buffer (pH 6.8). RNA concentration, 1.2 mM. Sample was measured for 2h at each temperature.

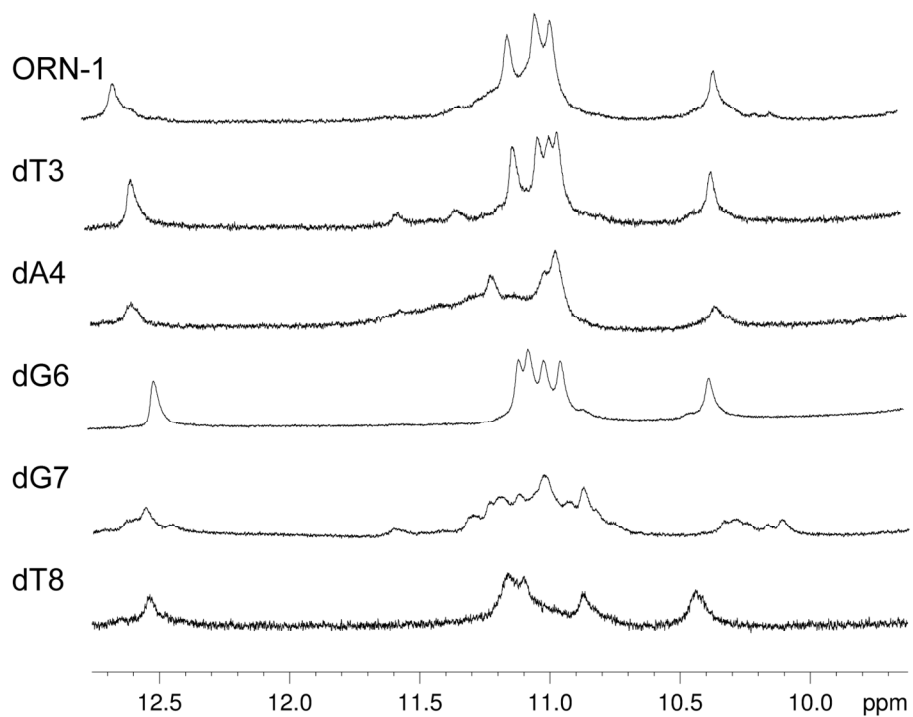


**Figure S3.** Imino proton NMR spectra of ORN-1 and the modified 8-nt human telomeric RNA sequences (Table S1) in Na<sup>+</sup> solution with deoxyribose substitutions. Experimental conditions: temperature, 25 °C; RNA concentration, ~1 mM.

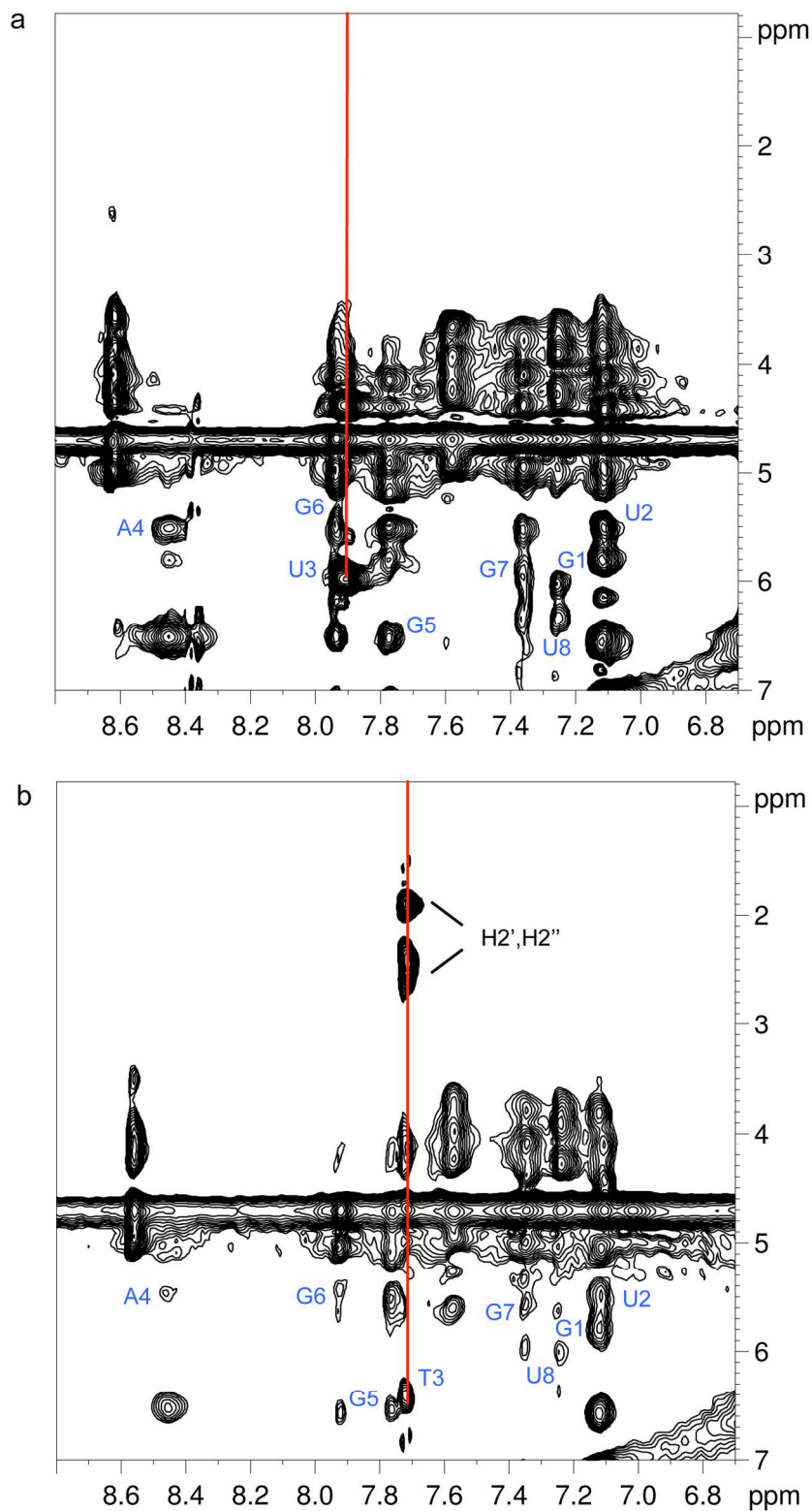


**Figure S4.** Example for the identification of the deoxyribose-substituted residue by upfield-shifted H2' and H2'' protons. NOESY spectra of (a) 8-nt ORN-1 sequence and (b) 8-nt modified sequence containing dT for rU substitution at position 3. Vertical lines (red) were traced for the U3(H6) and T3(H6). Each H8/6-H1' NOE peaks were marked with the corresponding position number.

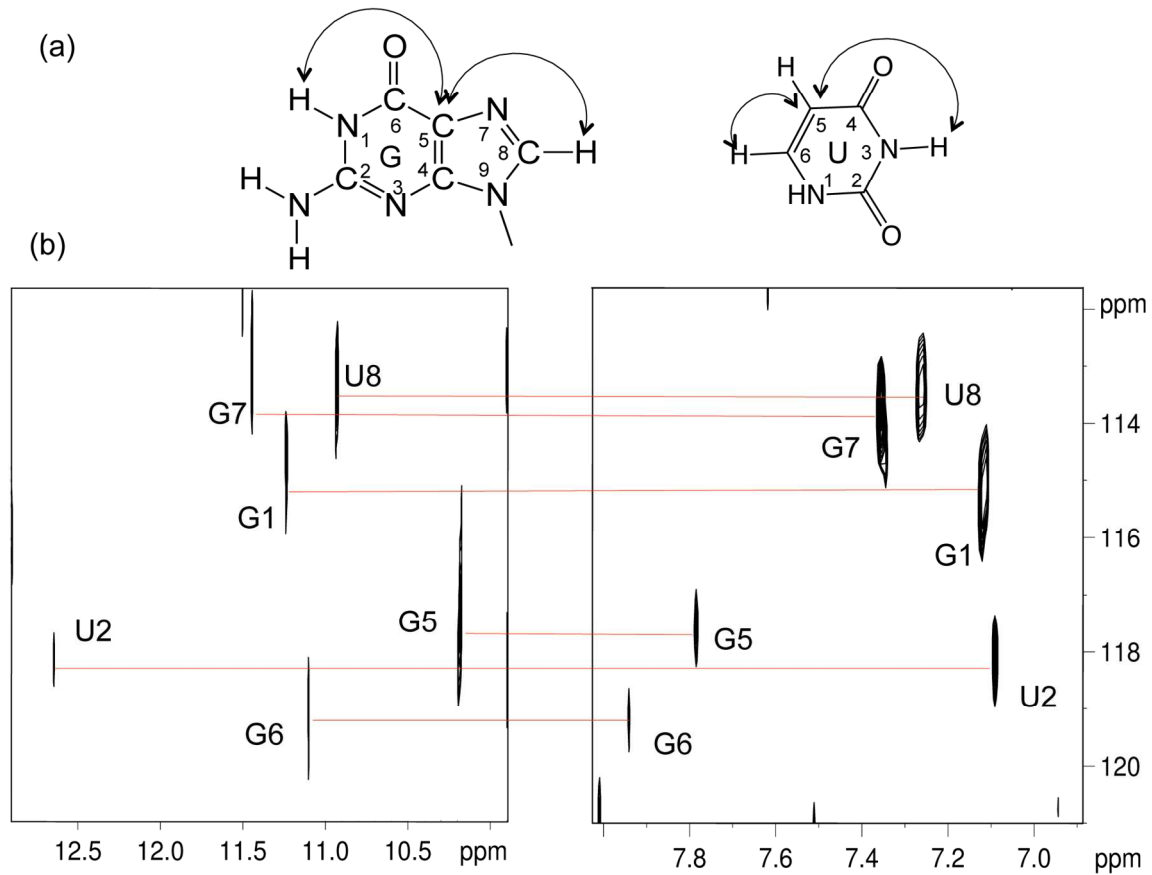


**Figure S5.** (a) The bases of rG and rU. Arrows indicate the coherence transfer pathways used in the experiments. Long-range J-couplings between imino and H8 protons via  $^{13}\text{C}5$  for rG, imino and H6 protons via  $^{13}\text{C}5$  for rU. (b) JR-HMBC spectra for 8-nt RNA. Through-bond correlations between imino and H8 protons via  $^{13}\text{C}5$  for rG, and imino and H6 protons via  $^{13}\text{C}5$  for rU, is at natural abundance. For the JRHMBC spectra 4096 scans per FID,  $\tau = 50$  ms, total measurement time of 122 h.

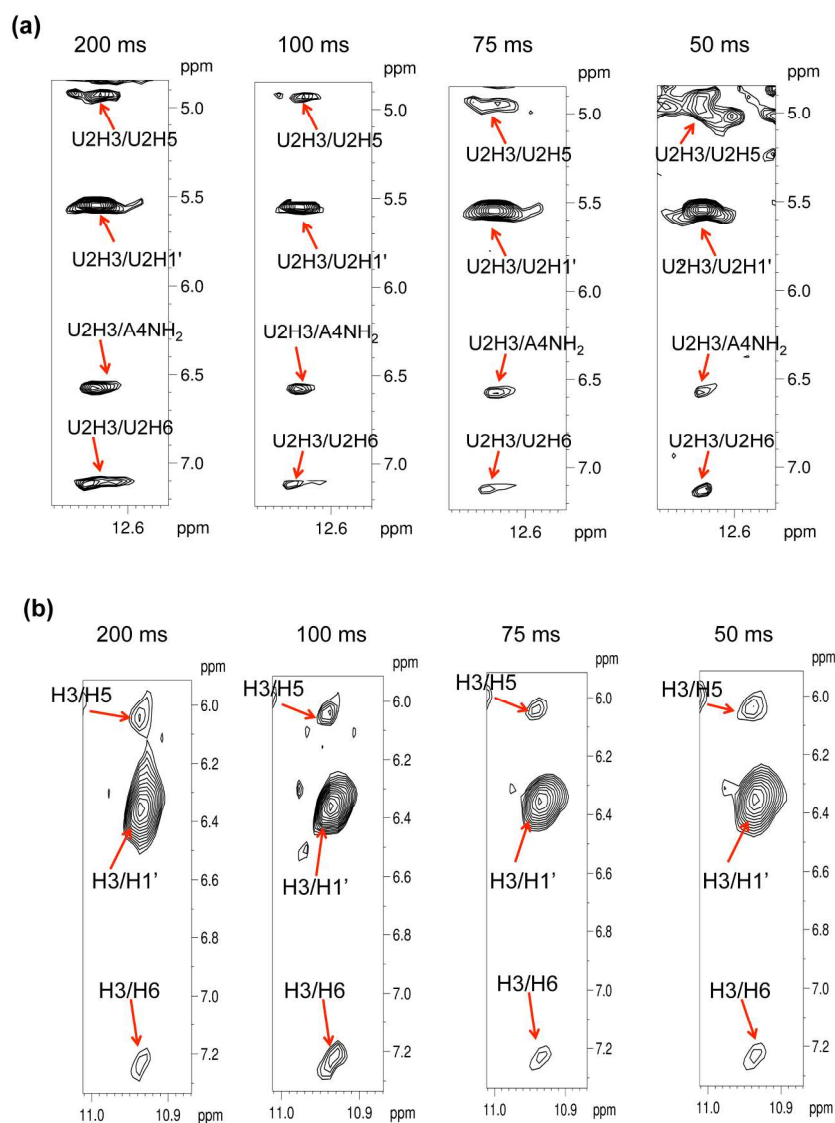


**Figure S6.** (a, b) The H3–H5/H6 (U2 and U8) proton region of NOESY spectra (a for U2, b for U8) of ORN-1 at different mixing times (shown at upper of spectra). Cross peaks for H3–H5 (U2 and U8), H3–H1' (U2 and U8) and H3–H6 (U2 and U8) are shown. Cross peak for U2H3–A4NH<sub>2</sub> is indicated. The H3/H5 and H3/H6 NOEs (U2 and U8) are observed at different mixing times, which indicates the NOEs of imino proton of U2 and U8 to H5 and H6 but not a result of spin diffusion, providing further evidence for the formation of U-tetrad.

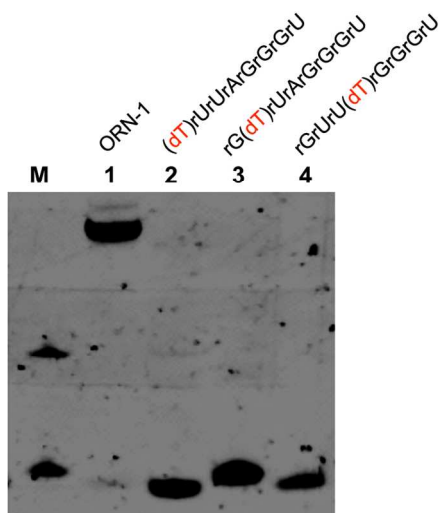


**Figure S7.** Denaturing gel electrophoresis of ORN-1. Lane M, markers dT12 and dT24; lane 1, ORN-1; lane 2, 3, and 4, the mutant ORN-1 sequences containing one thymidine substitution in G1, A4, and U2. The substituted thymidine is enclosed in brackets (red). The modified RNA sequences migrated slower faster than ORN-1, indicating that these RNA sequences do not adopt a higher order structure.

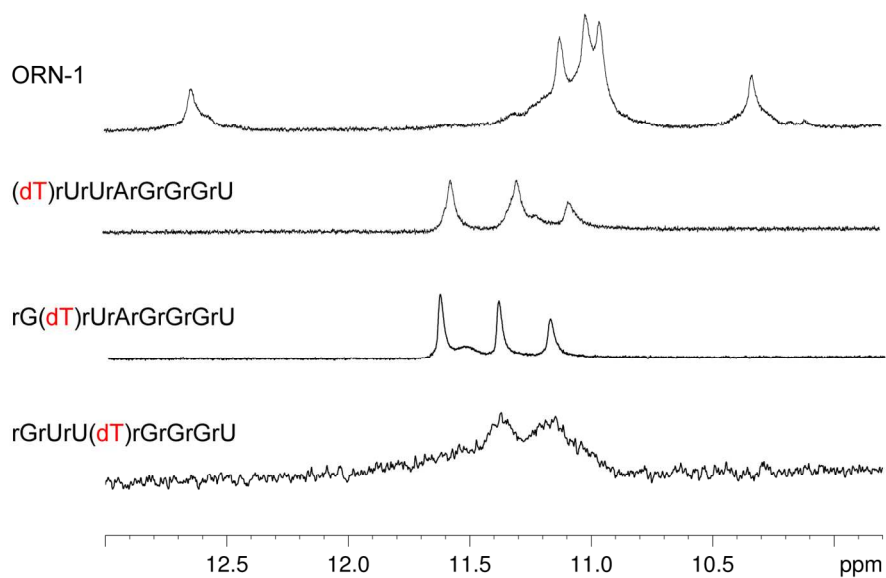


**Figure S8.** Imino proton NMR spectra of ORN-1 and the mutant sequences containing one thymidine substitution in G1, A4, and U2. The substituted thymidine is enclosed in brackets (red). The imino peaks of the mutant sequences in comparison to ORN-1 indicate that these substitutions perturb the overall higher order structure. Experimental conditions: temperature, 25 °C; RNA concentration, ~1 mM.

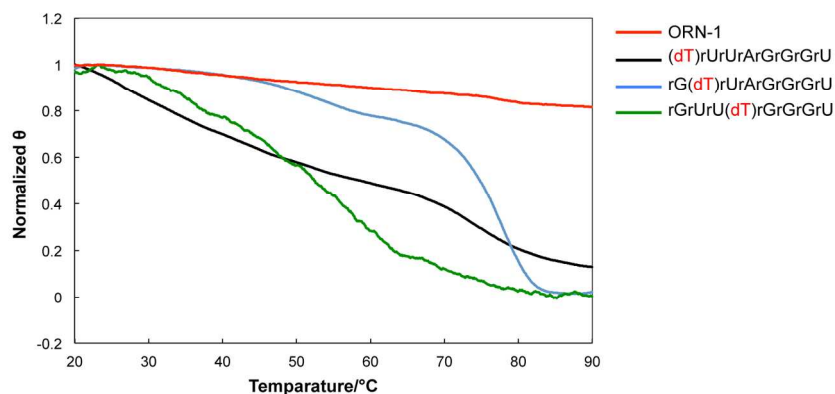


**Figure S9.** CD melting curves of ORN-1 and the mutant ORN-1 sequences containing one thymidine substitution in G1, A4, and U2 in 100 mM NaCl and 10 mM Tris-HCl buffer (pH 7.0). The substituted thymidine is enclosed in brackets (red). The modified RNA sequences have a different CD melting curve of ORN-1 with very low stability in comparison to ORN-1 indicated that the modifications affect the structure and stability of RNA.



**Figure S10.** Non-denaturing gel electrophoresis of ORN-1 at the low concentrations. Lane M, markers dT12 and dT24; lane 1, ORN-1 at 0.4  $\mu$ M; lane 2, ORN-1 at 0.8  $\mu$ M. We can still observe the higher order structure at the low concentrations (slower migration than the reference DNA oligonucleotide dT24), suggesting that the structure can form at the physiologically relevant concentrations.

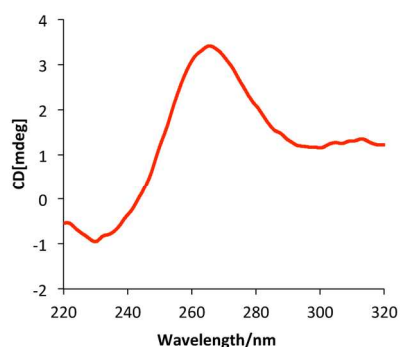


**Figure S11.** (a) CD spectrum of ORN-1 at the low concentration (1  $\mu$ M) in the presence of 100 mM NaCl at 25  $^{\circ}$ C. A positive band at 265 nm and a negative band around 240 nm, which are characteristics of CD spectra for parallel G-quadruplex structure, which suggested that the structure can form at the low concentration.

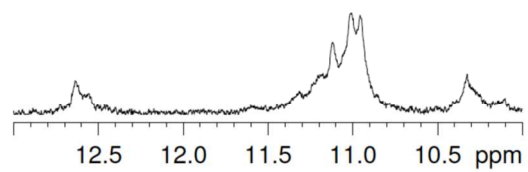


**Figure S12.** Imino proton NMR spectra of ORN-1 at the low concentration (0.1 mM) in Na<sup>+</sup> solution. Experimental conditions: temperature, 25 °C. The unchanged imino peaks indicate that the structure can form at the low concentration.

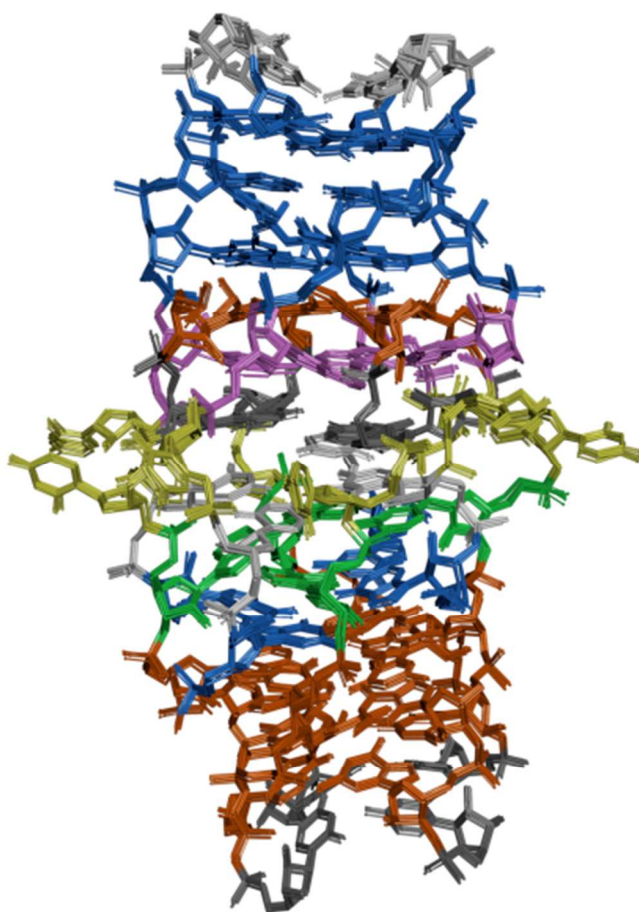


**Figure S13.** Structural model of ORN-1. Stereoviews of an ensemble of 10 lowest total energy structures.

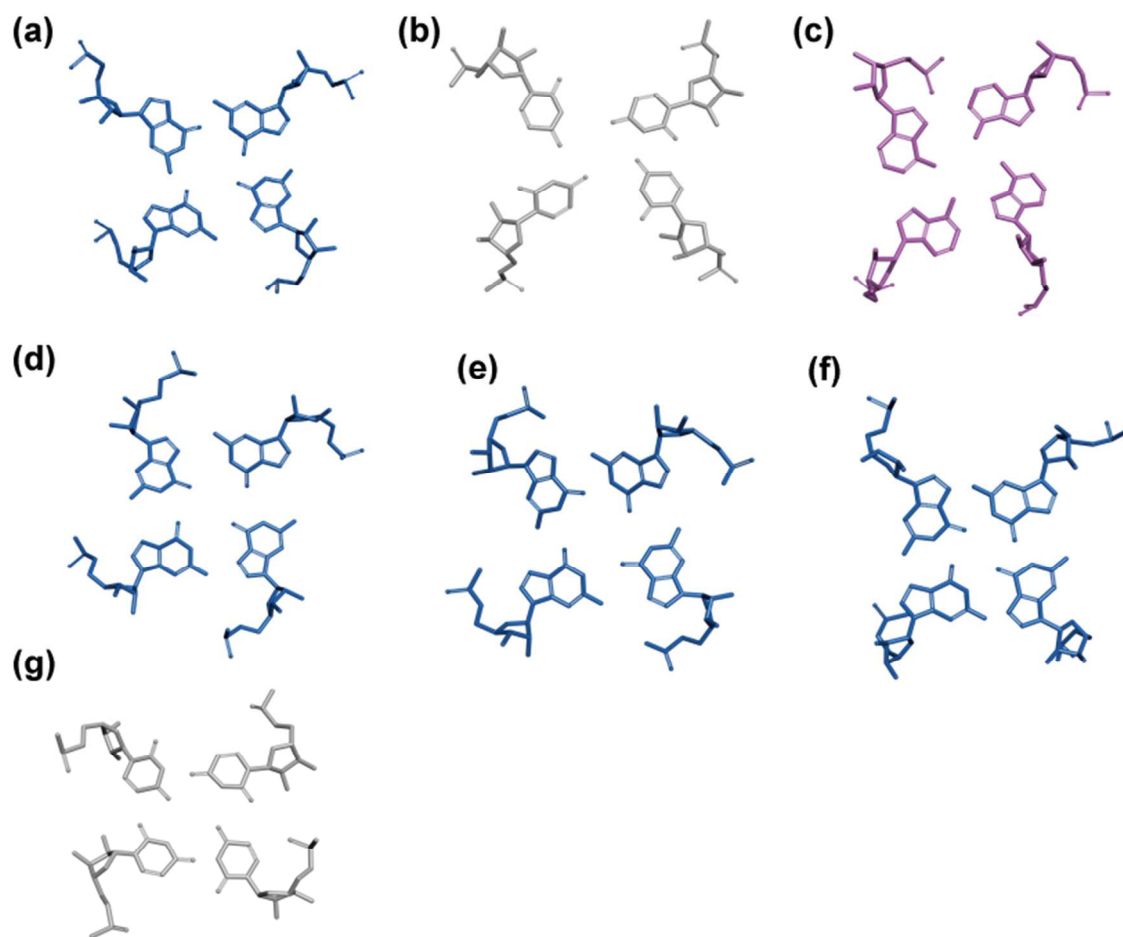


**Figure S14.** Base tetrad conformations. (a) G1, (b) U2, (c) A4, (d) G5, (e) G6, (f) G7, and (g) U8.

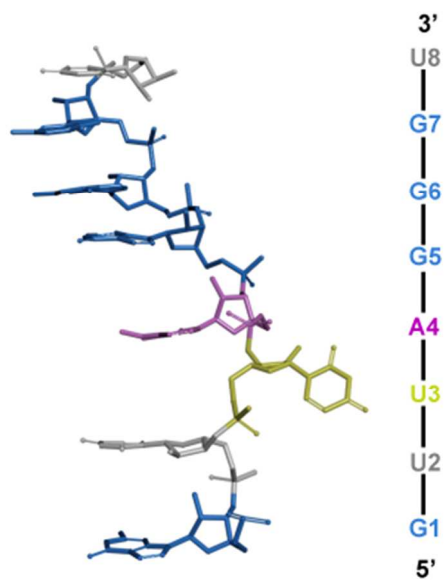


**Figure S15.** A stereoview of U3 (yellow) that is bulged out of the strand.

## Methods

**RNA Synthesis and Purification.** The syntheses of the RNAs were carried out by phosphoramidite chemistry. All RNAs were synthesized on the 1  $\mu$ mol scale with an automatic DNA/RNA synthesizer (Nihon Techno Service Co., LTD.). After automated synthesis, the oligonucleotides were detached from the support and deprotected according to the manufacturer's protocol. All oligonucleotides were purified by Reverse phase-HPLC (JASCO). RNA sequences are Table S1.

**CD Measurements and Analysis of CD Melting Profile.** CD spectra were measured using a Jasco model J-810 CD spectrophotometer. Samples were prepared by heating the oligonucleotides at 90 °C for 5 min and gradually cooling them to room temperature. The melting curves were obtained by monitoring at 265 nm CD band. Solutions for CD spectra were prepared as 0.3 mL samples at 1 – 10  $\mu$ M concentrations in the presence of 100 mM NaCl, 10 mM Tris buffer (pH 6.8).

**NMR Experiments.** NMR experiments were performed a BRUKER AVANCE 400 and 600 MHz spectrometer. A special Micro Tube that is designed for use with reduced sample volumes was used (catalog no: NE-H5/3-Br, New Era NMR). Spectra were recorded at 25 °C. RNA samples (0.1 – 5.2 mM) were dissolved in 0.15 mL of 90% H<sub>2</sub>O/10% D<sub>2</sub>O, 10 mM sodium phosphate buffer, pH 6.8, 100 mM NaCl. Assignments of the proton resonances were initially made by using the methods previously described for assignments of G-quadruplex RNA structures.<sup>1</sup> Site-specific ribose-to-deoxyribose substitutions, heteronuclear through-bond correlation experiments at the <sup>13</sup>C natural abundance [<sup>13</sup>C-<sup>1</sup>H] JR-HMBC, and homonuclear experiments, were used to assist spectral assignments. Resonance assignments of the remaining protons have been determined through a combination of 2D <sup>1</sup>H NOESY with various mixing times ranging from 50 to 300 ms.

**Gel Electrophoresis.** Nondenaturing gel electrophoresis experiment was performed on 20% polyacrylamide gel in a 1  $\times$  TBE buffer with the presence of 20 mM NaCl. Electrophoresis experiments were run at 80 V for 6 h at 4 °C, and the gel was viewed by GelStar (Lonza) staining. Samples at 0.4 – 100  $\mu$ M concentrations. DNA oligonucleotides dT12 and dT24 were used as molecular markers. Denaturing gel electrophoresis experiment was performed on 10 M urea/20% polyacrylamide gel in 1  $\times$  TBE buffer. The gel was viewed by GelStar (Lonza) staining.

**Molecular Modeling.** The model of G-quadruplex structure were manually generated based on the reported RNA G-quadruplex structure (PDB code 2M18 and 3IBK) using the BIOVIA Discovery Studio 4.5.

**NOE Restraints.** All assigned NOESY cross-peaks were classified to strong (1.8-3.0 Å), medium (1.8-3.7 Å), weak (1.8-5.5 Å) and very weak (1.8-7.5 Å) interproton distance restraints based on the intensity of NOESY. The NOE peaks of H5-H6 from uracil bases were used as calibration for the distance measurements. Distance restraints for the hydrogen bonding in each tetrad were 1.8-3.0 Å. For each G, A, and U2-Tetrad, three dihedral restraints were applied to maintain the plane structure with a force constant of 50 kcal mol<sup>-1</sup>Å<sup>-2</sup>. The force constant of hydrogen bonds and NOE restraints were kept between 5 to 50 kcal mol<sup>-1</sup>Å<sup>-2</sup> throughout the computation.

Then molecular dynamics simulations were performed by the standard dynamics cascade in BIOVIA Discovery Studio 4.5 with some modifications. Generally, the structure was heating from 50 K to 300 K over 4 ps and equilibration at 300 K with 100 ps simulation time. The save results interval in the production step was 2 ps during 100 ps simulation time at 300 K. 10 best conformations generated by simulation were further energy minimized until the gradient of energy was less than 0.1 kcal · mol<sup>-1</sup>. The conformation with lowest energy was selected as shown in Figure 4.

1. Martadinata, H.; Phan, A. T., Structure of propeller-type parallel-stranded RNA G-quadruplexes, formed by human telomeric RNA sequences in  $K^+$  solution. *J. Am. Chem. Soc.* **2009**, *131*, 2570.